

Provided for non-commercial research and education use.
Not for reproduction, distribution or commercial use.



This article appeared in a journal published by Elsevier. The attached copy is furnished to the author for internal non-commercial research and education use, including for instruction at the authors institution and sharing with colleagues.

Other uses, including reproduction and distribution, or selling or licensing copies, or posting to personal, institutional or third party websites are prohibited.

In most cases authors are permitted to post their version of the article (e.g. in Word or Tex form) to their personal website or institutional repository. Authors requiring further information regarding Elsevier's archiving and manuscript policies are encouraged to visit:

<http://www.elsevier.com/copyright>



Contents lists available at ScienceDirect

Earth and Planetary Science Letters

journal homepage: www.elsevier.com/locate/epsl

Turbulent mixing in the Amazon River: The isotopic memory of confluences

Julien Bouchez^{a,*}, Eric Lajeunesse^b, Jérôme Gaillardet^a, Christian France-Lanord^c, Poliana Dutra-Maia^d, Laurence Maurice^d^a Institut de Physique du Globe de Paris, Equipe de Géochimie-Cosmochimie - Université Paris Diderot, 4 place Jussieu 75252 Paris cedex 05, France^b Institut de Physique du Globe de Paris, Equipe de Dynamique des Fluides Géologiques - Université Paris Diderot, 4 place Jussieu 75252 Paris cedex 05, France^c Centre de Recherches Pétrographiques et Géochimiques - Centre National pour la Recherche Scientifique, 15 rue Notre-Dame-des-Pauvres, 54501 Vandœuvre-lès Nancy, France^d Laboratoire des Mécanismes de Transfert en Géologie - Institut de Recherche pour le Développement - Université de Toulouse Paul Sabatier, 14 avenue Edouard Belin, 31400 Toulouse, France

ARTICLE INFO

Article history:

Received 6 April 2009

Received in revised form 12 November 2009

Accepted 26 November 2009

Available online 31 December 2009

Editor: M.L. Delaney

Keywords:

Amazon River
confluence
Sr isotopes
turbulent mixing
dissolved species
heterogeneities

ABSTRACT

Rivers continuously discharge dissolved material to the oceans. Dissolved compounds partially result from water–rock interactions, which produce a large range of water chemical and isotopic compositions. These waters are collected by rivers, that are commonly assumed to be well-mixed with regard to their different tributaries, as a result of turbulent dispersion. In this paper, we test this hypothesis on the Solimões River (at Manacapuru), the largest tributary of the Amazon River, by analyzing the sodium concentration and strontium isotopic composition of river water on a transverse section at different depths. High-precision measurements reveal lateral heterogeneities. This reflects poor mixing between two main river masses, that have distinct chemical and isotopic signatures, a hundred kilometers downstream from their confluence: the Solimões mainstream and the Purús River. Using sodium concentration data, the transverse dispersion coefficient is estimated for the studied Solimões reach (the Earth's largest river on which such an estimate now exists), and is found to be $1.8 \pm 0.2 \text{ m}^2/\text{s}$. Comparison with previously reported data highlights the potential role of bed morphology and islands in the efficiency of lateral mixing in large rivers. We finally demonstrate that the characteristic length of lateral mixing downstream from confluences in large rivers is at least of several tens of kilometers.

© 2009 Elsevier B.V. All rights reserved.

1. Introduction

At Earth's surface, water–rock interactions taking place under various geological, climatic and ecological conditions, generate a broad spectrum of river water compositions (Stallard and Edmond, 1983; Huh et al., 1998; Gaillardet et al., 1999). Large rivers collect waters that have distinct chemical and isotopic signatures, originating from drastically different geographical areas.

Given their high Reynold's number (10^6 to 10^8), rivers flow under a turbulent regime. In this regime, the flow is characterized by large fluctuations of velocity entraining a macroscopic random movements of fluid particles (Csanady, 1973; Tritton, 1988; Pope, 2008). These fluctuations act on a large range of length and time scales, and tend to homogenise river water compositions with an efficiency much larger than what is expected from molecular diffusivity alone. Still turbulent mixing acts at a finite rate that might be sufficiently slow for chemical heterogeneities to persist in natural systems (Mackay, 1970; Stallard, 1987; Rathbun and Rostad, 2004). Turbulent dispersion rates, especially lateral dispersion rates, are still poorly constrained on natural systems (e.g. Fischer, 1973, 1976; Yotsukura and Sayre, 1976;

Rutherford, 1994; Gaudet and Roy, 1995), although they are of great importance for the fate of water masses in confluences, the issue of collecting representative river water samples, and the dispersion of pollutants. Most studies on both experimental and natural systems are based on the release of dye tracers at a given position of the flow, and on the rate of the spreading of this dye (Caplow et al., 2004). Alternatively, dissolved chemical compounds naturally present in rivers can be used to trace water masses and their mixing (Stallard, 1987). The use of such natural geochemical tracers to study mixing rates in large rivers relies on several prerequisites: (i) the two tributaries must have distinct chemical signatures (ii) the two tributaries must have comparable water discharges (for the preservation of both signatures relatively far downstream) (iii) the confluence must be relatively close to the sampling point. In this perspective, the analytical precision on the considered natural chemical tracer is critical and determines its ability in distinguishing between two water masses of potentially close chemical signatures. The tracer also has to be conservative: the behavior of dissolved major elements and heavy metals under changing contents of dissolved organic matter in continental waters, occurring for example at confluences between organic-rich and sediment-rich rivers, has shown in many cases to be non-conservative (Aucour et al., 2003; Moreira-Turcq et al., 2003; Maurice-Bourgoin et al., 2007a). This is especially true for elements involved in exchange reactions between

* Corresponding author. Tel.: +33 1 44 27 48 16; fax: +33 1 44 27 49 16.
E-mail address: bouchez@ipgp.jussieu (J. Bouchez).

mineral and organic surfaces or present in water as colloids, and not truly dissolved (Dupré et al., 1999). As shown by these studies, sodium and chloride suffer least from such interactions. Isotopic ratios of heavy elements, such as strontium, bypass the problems arising by the use of major elements. The small relative difference of mass between the two isotopes of Sr, ^{86}Sr and ^{87}Sr , makes Sr isotopic ratio $^{87}\text{Sr}/^{86}\text{Sr}$ insensitive to physical and chemical interactions, thus a perfect source proxy. This approach has been extensively used to trace mixing in different geological materials, in particular Earth's mantle chemical heterogeneities (Allègre et al., 1987). Moreover, Sr isotopic ratios can be measured with a relative precision better than 10^{-5} , due to recent progress in mass spectrometry, allowing for the detection of very small proportions of mixing, even if the different water masses have slightly distinct compositions. Finally, Sr isotopic ratios are well-suited as water source tracers in large rivers because continental provinces of different mean geological ages display contrasted Sr isotopic ratios.

In this contribution, we report chemical and Sr isotopic analyses on a river cross-section of the Solimões River, the largest tributary of the Amazon River. Data show that the river is not laterally homogenous, and allow to calculate the lateral dispersion coefficient. The results of this study, along with literature data, demonstrate that most large rivers are heterogeneous when they discharge into the oceans. We discuss the importance of a number of geomorphological and hydrological factors on influencing the lateral mixing efficiency downstream from a confluence of large rivers.

2. Sampling site and analytical methods

The Amazon River transports $6600 \text{ km}^3/\text{yr}$ of water and 290 MT/yr of dissolved material to the oceans. The Solimões River contributes 192 MT/yr to this load (Molinier et al., 1996; Meybeck and Ragu, 1996; Gaillardet et al., 1997). The different geologic units drained by the Amazon River (which catchment area is 6 million km^2) generate different types of waters. The Solimões and Madeira rivers, derived from the Andes, are “white water” rivers, having both high dissolved and particulate concentrations (Stallard and Edmond, 1983; Sioli, 1984). Rivers draining only the low-relief and forested areas are either “black water” or “clear water” rivers, with low inorganic dissolved content and low suspended particles concentrations (Gibbs, 1967). $^{87}\text{Sr}/^{86}\text{Sr}$ in the Amazon basin waters ranges from 0.709 in the Andean tributaries to 0.733 in the lowland tributaries. The occurrence of young volcanic rocks in the Andes constitutes a source of relatively

^{86}Sr -enriched strontium, as opposed to the radiogenic strontium of the Amazon lowlands (Goldstein and Jacobsen, 1984; Gaillardet et al., 1997).

The Solimões River was sampled on 25 March 2006 at the Manacapuru cross-section before its confluence with the Negro River (Fig. 1). This section is known as a representative gauging station of the Solimões, far from large tributaries influence. Acoustic Doppler Current Profiler (ADCP, Rio Grande RD Instruments, frequency 600 kHz) was used to map the river bottom and obtain accurate discharge and water velocity structure data (Filizola and Guyot, 2003). Then, three sampling verticals were made, distributed along the cross-section, and on each of these verticals, three to five samples of river water were taken, leading to a “grid” covering the river cross-section. Eight liters of water were taken by submerging a point-sediment sampler (University of Manaus) down to the wanted depth, with an uncertainty of about a meter. After sample recovery, under-pressure Teflon filtration unit (PSE filter sheets, $0.22 \mu\text{m}$) were used for on-board filtration. The first two filtrated liters of water were discarded, and the third was stored at pH 2 in pre-acid-washed polypropylene bottles for dissolved phase analysis. Samples and their main characteristics are listed in Table 1. Sodium (Na^+) concentrations were measured by ion chromatography at the Institut de Physique du Globe de Paris, France. Relative external reproducibilities were lower than 3% (2σ). Sr concentrations were obtained by ICP-MS at IPGP, using In as an internal standard (Dupré et al., 1996). Relative external reproducibilities were better than 5% (2σ). Approximately 500 ng of Sr were separated from the matrix by ion chromatography (Meynadier et al., 2006), and Sr isotopic compositions were measured by MC-TIMS Triton (Thermo-Finnigan) at IPGP (Birck, 1986). The blank of the chemical procedure was evaluated to be a few hundreds of pg, and the relative external reproducibility to be lower than 10^{-5} (2σ).

3. Results

Dissolved species concentrations measured in this study compare well with the results reported by Stallard and Edmond (1983), Gerard et al. (2003), Seyler and Boaventura (2003), Mortatti and Probst (2003) and Viers et al. (2005). Na^+ concentrations in vertical profile # 1 (sampled 975 m from the left bank) are around $130 \mu\text{mol/L}$, with a slight downward decrease (Table 1, Fig. 2). On the other hand, profile # 3 (sampled 2550 m from the left bank) has lower Na^+ concentrations (around $95 \mu\text{mol/L}$) and displays a slight downward increase. The

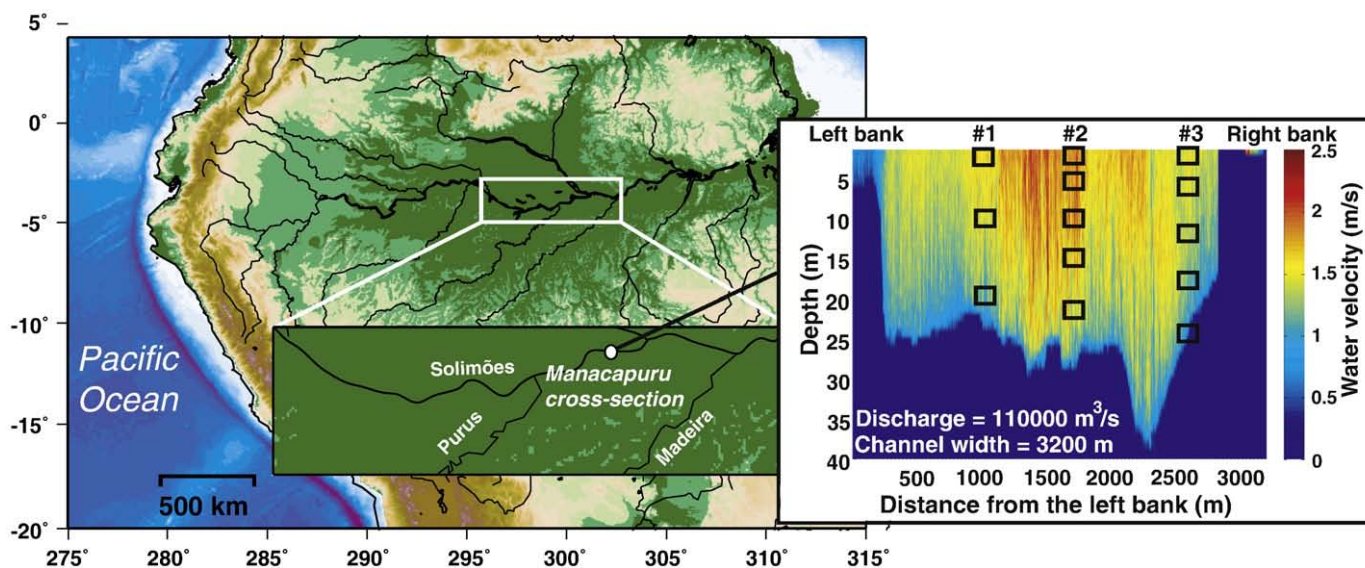


Fig. 1. Map of the Amazon River basin and location of the Manacapuru sampling cross-section. The ADCP velocity transect is shown, on which samples are represented by rectangles.

Table 1

Samples list, characteristics, Na⁺ and Sr concentrations, and Sr isotopic composition. ND: not determined. Relative analytical uncertainties are better than 3% for Na⁺, better than 10% for Sr, and better than 10⁻⁵ for ⁸⁷Sr/⁸⁶Sr (2σ).

Sample	Profile #	Sampling depth (m)	Longitude (W)	Latitude (S)	Distance from the left bank (m)	Total depth (m)	Na ⁺ (μmol/L)	Sr (ppb)	⁸⁷ Sr/ ⁸⁶ Sr
AM-06-07	1	20	60°33'12.0"	03°18'42.1"	975	24	127	72	0.709033
AM-06-08	1	10	60°33'12.0"	03°18'42.1"	975	24	133	68	0.709040
AM-06-09	1	0	60°33'12.0"	03°18'42.1"	975	24	132	67	0.709034
AM-06-10	2	22	ND	ND	1675	25	124	63	0.709075
AM-06-11	2	15	ND	ND	1675	25	124	63	0.709070
AM-06-12	2	10	ND	ND	1675	25	123	59	0.709064
AM-06-13	2	5	ND	ND	1675	25	122	ND	0.709063
AM-06-14	2	0	ND	ND	1675	25	123	62	ND
AM-06-15	3	25	60°33'11.0"	03°19'41.0"	2550	27	101	46	0.709183
AM-06-16	3	18	60°33'11.0"	03°19'41.0"	2550	27	98	47	0.709214
AM-06-17	3	12	60°33'11.0"	03°19'41.0"	2550	27	97	44	0.709204
AM-06-18	3	6	60°33'11.0"	03°19'41.0"	2550	27	96	45	0.709202
AM-06-19	3	0	60°33'11.0"	03°19'41.0"	2550	27	98	45	0.709130

"intermediate" profile (#2, sampled 1675 m from the left bank) exhibits intermediate and rather constant Na⁺ concentrations (120–125 μmol/L). The total variation throughout the cross-section (35 μmol/L, or 30% of relative variation) is about ten times the analytical reproducibility and is therefore significant.

Besides the slight variation of ⁸⁷Sr/⁸⁶Sr within the profile #3, the observed overall trend is a gradient from low (around 0.709040) Sr isotopic ratios in the profile which is the closest to the left bank (# 1), towards more radiogenic values near the right bank (profile # 2, ⁸⁷Sr/⁸⁶Sr around 0.709080, then profile # 3, ⁸⁷Sr/⁸⁶Sr around 0.709200; Table 1, Fig. 2). The total variation of dissolved Sr isotopic ratios found in the Solimões vertical depth-profiles is of about 200 × 10⁻⁶. This range is about thirty times the analytical reproducibility and therefore more significant than the Na⁺ variations.

4. Discussion

4.1. Cause of the observed heterogeneity

Sodium and strontium data both demonstrate (i) the vertical homogeneity and (ii) the existence of lateral water heterogeneities within the Solimões River cross-section. The possibility that chemical concentra-

tions could be affected by exchange with colloids (Dupré et al., 1999) or solids not evenly distributed through the river transect can be discarded (Maurice-Bourgoin et al., 2007b), based on the isotopic heterogeneities of a heavy element such as Sr. The Sr isotopic ratio is correlated with the inverse of Sr concentration (Table 1, Fig. 3). In such a diagram, a straight line can be interpreted as a mixing trend. The non-radiogenic end-member can be accounted for by the Solimões mainstream (Gaillardet et al., 1997), whereas the radiogenic end-member is likely water originating from lowland regions. For example, a sample from the Negro River, which is a strictly lowland tributary of the Amazon River, yielded a ⁸⁷Sr/⁸⁶Sr of 0.72734 ± 10⁻⁵. The lower Na⁺ concentration in the radiogenic end-member (Fig. 2) also indicates a lowland source (Stallard and Edmond, 1983; Sioli, 1984; Gaillardet et al., 1997). The observed lateral heterogeneities thus indicate the occurrence of two water masses coming from different sources (Fig. 4).

4.2. Origin of the radiogenic end-member

It is impossible to distinguish two water masses at the Manacapuru sampling site, neither on the field nor from satellite images or aerial shots (Fig. 4); it is thus not straightforward to identify the source of the radiogenic end-member, unlike in other cases where obviously

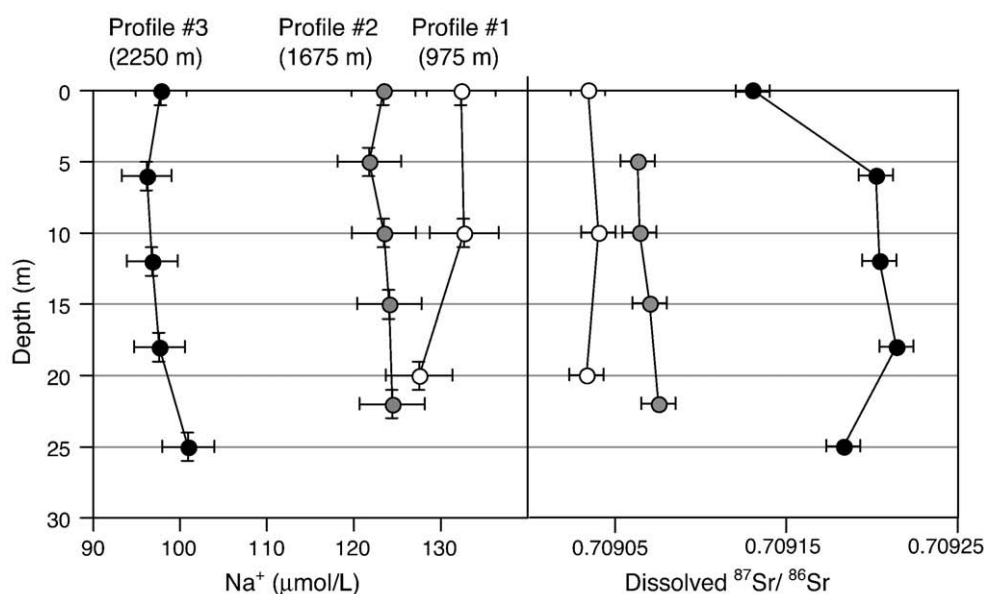


Fig. 2. Na⁺ concentrations and Sr isotopic ratios vs. depth at Manacapuru, Solimões River, for the three vertical profiles. White, grey and black circles are samples from profiles # 1, # 2 and # 3, as indicated above Na⁺ concentrations. Distances from the left bank are also indicated.

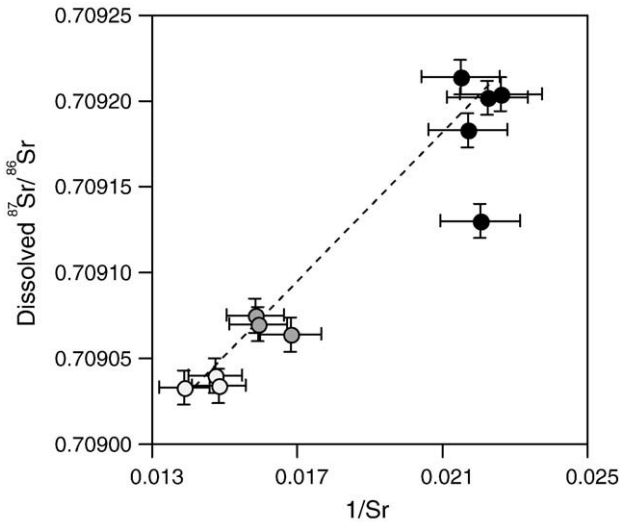


Fig. 3. $^{87}\text{Sr}/^{86}\text{Sr}$ vs. $1/\text{Sr}$ in the Manacapuru cross-section, Solimões River. Symbol colors have the same meaning as in Fig. 2.

contrasting water masses mix (Mackay, 1970; Rathbun and Rostad, 2004). In our case, only the chemical and isotopic heterogeneities can be used to identify the nature of the source of the water masses. There are different candidates for the radiogenic end-member: (i) a small “black water” tributary, the Manacapuru River, joins the Solimões ca. ten kilometers upstream from the sampling location; (ii) an important tributary, the Purús River, draining the right-bank floodplain, discharges into the Solimões 100 km upstream the sampling location; (iii) groundwater seepage and/or floodplain lake outputs (Fig. 4).

The highest Sr isotopic ratios are obtained near the right bank of the studied cross-section; they thus cannot be due to the supply of water by the small Manacapuru River (likely having radiogenic dissolved Sr), which reaches the Solimões along the left bank. Moreover, the discharge of the Manacapuru River is negligible compared to the Solimões mainstream (Filizola, 2003), and is obviously unable to quantitatively account for the variation observed in the Solimões river cross-section. Groundwaters are unlikely to display different Sr isotopic composition from one bank to another, and the large mainstream discharge at the time of sampling ($110,000 \text{ m}^3/\text{s}$) precludes any significant supply of Sr by seepage of from floodplain lakes (Maurice-Bourgoin et al., 2007b). We therefore propose that the variability observed in the Manacapuru cross-section is inherited from the supply of relatively radiogenic Sr water from the Purús River to the Solimões River, and from the lack of lateral mixing between these two water masses. Although there is no published data on the dissolved $^{87}\text{Sr}/^{86}\text{Sr}$ of the Purús River to our knowledge, previously reported concentrations for major elements concentrations using data from the CAMREX program (Mortatti and Probst, 2003) tend to show that the Purús River is relatively diluted, thus probably having chemical characteristics close to those of a lowland river.

4.3. Determination of the lateral turbulent dispersion coefficient

Although it is particularly important for predicting heterogeneities persistence and pollutants spreading in rivers, no sound theoretical basis exists to describe turbulent mixing (Gualtieri, 2009). The prediction of its rate still relies on semi-empirical models deduced from experimental investigations performed in laboratory channels and in natural streams. Observations show that the random motion of fluid particles in a turbulent flow diffuses dissolved compounds inside a fluid in much the same way that thermal agitation gives rise to molecular diffusion (Pope, 2008; Gualtieri, 2009). Within the frame of this analogy, turbulent mixing is usually modelled by a diffusive law;

the flux F_i (in $\text{mol m}^{-2} \text{ s}^{-1}$) of a dissolved element i transported by turbulent diffusion along the lateral direction can thus be written as (Taylor, 1954):

$$F_i = -\varepsilon_y \times \frac{\partial C_i}{\partial y}, \quad (1)$$

where C_i is the concentration of the element i (in mol m^{-3}) and ε_y is the turbulent diffusion coefficient along the y cross-channel coordinate, or lateral turbulent diffusion coefficient (in $\text{m}^2 \text{ s}^{-1}$). Turbulence operates on length scales much larger than thermal agitation and ε_y is therefore orders of magnitude larger than molecular diffusion coefficient. However, contrary to the case of molecular diffusion, ε_y is not an intrinsic property of the fluid but depends on the characteristics of the turbulent flow (see Sec. 4.4). Because of the lack of theoretical description of turbulence, the determination of ε_y and of its variation with various hydrodynamical and geomorphological factors is still a matter of debate, as discussed with more details in the next section. In the present section, we use our data to estimate the lateral turbulent dispersion coefficient in the Solimões River, between the Solimões–Purús confluence and the Solimões mouth.

A 1-D, depth-integrated, direct modelling of the diffusion profile of any dissolved compound along the lateral direction can be made using Eq. (1) together with the mass conservation equation. Due to the lack of constraints on the Purús Sr isotopic composition, we chose to model the diffusion of Na^+ downstream of the Solimões–Purús confluence, and the resulting Na^+ concentration lateral profile at the Manacapuru sampling site. The aim of this modelling is to test the theoretical Na^+ concentration profile against our data at the Manacapuru sampling site, so as to determine the value of ε_y . To model the diffusion of Na^+ along the transverse direction y with time t , the following equation is solved for Na^+ concentration:

$$\frac{\partial [\text{Na}^+]_{\text{int}}}{\partial t} = \varepsilon_y \frac{\partial^2 [\text{Na}^+]_{\text{int}}}{\partial y^2}, \quad (2)$$

$[\text{Na}^+]_{\text{int}}$ being the depth-integrated Na^+ concentration. This equation is then non-dimensioned to:

$$\frac{\partial C}{\partial T} = \frac{\partial^2 C}{\partial Y^2}, \quad (3)$$

with :

$$T = \frac{\varepsilon_y}{W^2} t, \quad Y = \frac{y}{W}, \quad C = \frac{[\text{Na}^+]_{\text{int}}}{[\text{Na}^+]_{\text{ref}}}, \quad (4)$$

with W the river width (assumed to remain constant over the whole reach) and $[\text{Na}^+]_{\text{ref}}$ the mean Na^+ concentration measured in profile #1 at the Solimões sampling site. The boundary conditions are:

$$\left(\frac{\partial C}{\partial Y}\right)_{Y=0} = \left(\frac{\partial C}{\partial Y}\right)_{Y=1} = 0, \quad (5)$$

i.e. no sodium enters the channel through banks. Observation of satellite images (e.g. Fig. 4) shows that, at the Solimões–Purús confluence, the blackish Purús water mass is confined to ca. 15% of the total river width. This water mass has the Na^+ concentration of the Purús, that we take as the reported decadal mean (Mortatti and Probst, 2003). Hence, the initial conditions are $C(t=0, Y) = 0.53$ for Y between 0 and 0.15 and $C(t=0, Y) = 1$ for Y between 0.15 and 1.

Eq. (3) is solved analytically (Farlow, 1993). Then, different values of T (corresponding to different values of ε_y) are tested in the solution equation. The best agreement between modelled and measured Na^+ concentration profile was found for $T = 0.0140 \pm 0.0015$ (RMSE = 0.03), which corresponds to $\varepsilon_y = 1.8 \pm 0.2 \text{ m}^2 \text{ s}^{-1}$. The C profile is plotted, along with samples, in Fig. 5 as a function of Y , for $T=0$ (corresponding to

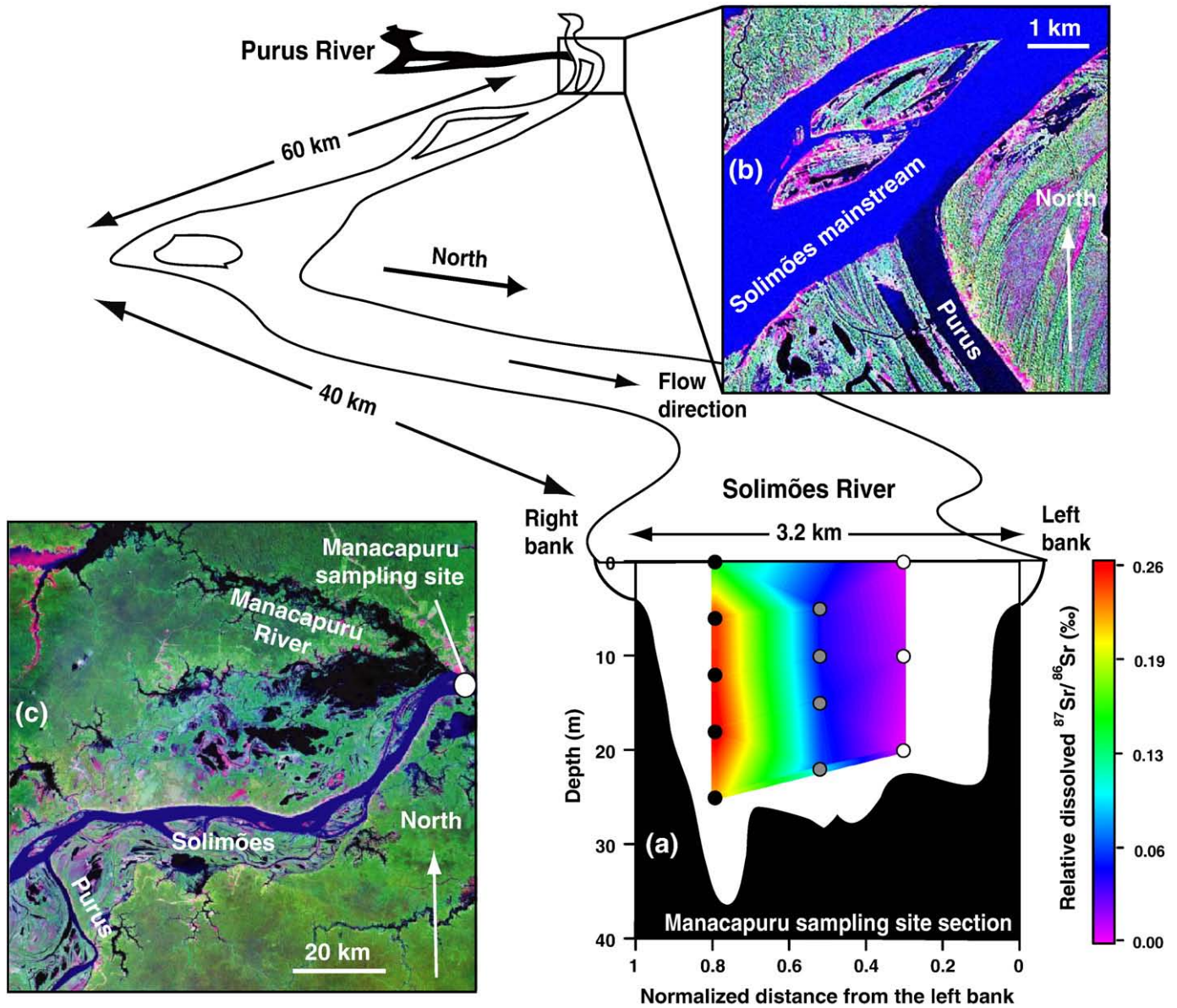


Fig. 4. (a) Sr isotopic ratios in the Solimões cross-section. Sr isotopic ratios are given in relative deviation compared to 0.709033 (in ‰), which is the smallest value obtained for this sampling site, and which is interpreted as the “mainstream” end-member. Spatial interpolation of Sr isotopic ratios between samples is obtained by a Delaunay triangulation. The main features of the hydrographic network upstream the sampling location are also shown. (b) Landsat image of the Solimões–Purús confluence, showing the blackish contribution of the tributary to the mainstream near the confluence. (c) Landsat image of the whole studied reach.

the confluence) and $T = 0.0140 \pm 0.0015$. This calculation of ϵ_y makes the Solimões the world's largest river on which an estimate of the lateral turbulent dispersion coefficient now exists.

4.4. Comparison with literature data

Following arguments analog to the Prandtl mixing length theory, dimensional reasoning suggests to relate the lateral turbulent mixing coefficient to turbulent length and velocity scales, respectively L and U , as (Pope, 2008; Gualtieri, 2009):

$$\epsilon_y \approx \alpha \times U \times L. \quad (6)$$

where α is a constant which depends on the river geometry as discussed hereafter.

Measurements performed on natural rivers and experimental channels support Eq. (6) (Fischer et al., 1979; Rutherford, 1994) and suggest to take the bed shear velocity u^* as the characteristic velocity

scale U . u^* is indeed linked to the turbulent shear stress τ exerted by the river on its bed by $\tau = \rho u^{*2}$ (with ρ the density of the fluid). Therefore u^* provides a good estimate of the mean intensity of velocity fluctuations (in any direction) in a turbulent flow (Tritton, 1988; Pope, 2008).

In a river, the vertical mean velocity profile $u(z)$, where z is the height above the river bed, follows the so-called law of the wall (Vanoni, 2006):

$$\frac{u(z)}{u^*} = \frac{1}{\kappa} \cdot \log\left(\frac{z}{z_0}\right), \quad (7)$$

where κ is the Von Kármán constant, equal to 0.41 (Vanoni, 2006), and z_0 the bed roughness length. Fitting the ADCP water velocity vertical profiles by Eq. (7) thus allows to estimate u^* (Fig. 6). A very low u^* value was obtained for the profile #1, owing to the overall relatively constant water velocity over channel depth. This result was discarded because of the large uncertainty associated to its estimate.

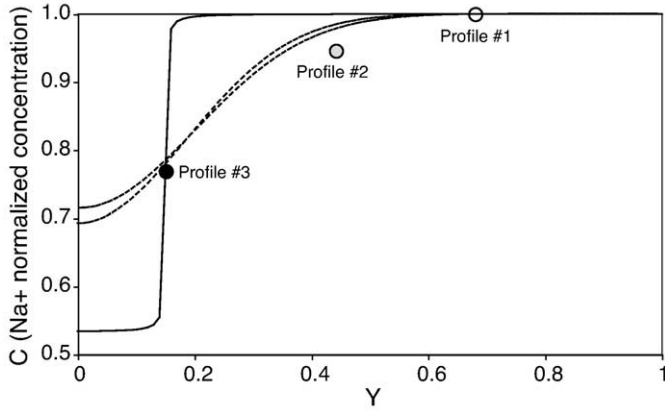


Fig. 5. Modelling of the Na^+ concentration profile, along with samples (each dot represents the arithmetical mean of Na^+ concentration over one depth-profile). Symbol colors for samples are the same as in Figs. 2 and 3. The solution of Eq. (3) (modelled Na^+ profile) is a Fourier series. The first 200 terms were used to calculate the numerical solution. The plain line is the modelled Na^+ concentration at the Purús-Solimões confluence, the two dashed lines are the modelled Na^+ concentration at the sampling site for the range of T (adimensioned time elapsed between confluence, see text for details) for which the agreement is the best between model and data.

Profiles # 2 and # 3 respectively yielded 0.03 m s^{-1} and 0.06 m s^{-1} for u^* . These results are consistent with shear bottom velocity calculated through $u^* = \sqrt{gHS}$, where g is the gravitational acceleration, H channel depth and S the water surface gradient. Using previously reported radar altimetry data (Dunne et al., 1998), which gives values for S at Manacapuru in the range $2\text{--}4 \cdot 10^{-5}$, u^* values in the range $0.07\text{--}0.10 \text{ m s}^{-1}$ are calculated, consistently with results of Eq. (7). Considering these estimates, u^* at the Manacapuru cross-section was finally taken as 0.05 m s^{-1} . We assume that this value, stemming from a local fit, applies to the whole section studied here.

The characteristic length scale L of Eq. (6) is still a matter of debate (Rutherford, 1994; Gualtieri, 2009). Fischer et al. (1979) considers that the mean flow depth H is the characteristic length scale, while recognizing that α varies slowly with the aspect ratio of the channel, implying a dependency of ε_y on the channel width. Following this approach, we consider that the mean flow depth, *i.e.* 25 m for Manacapuru, is the characteristic length scale of the turbulent dispersion coefficient. Using determined u^* and H in Eq. (6) yields $\alpha \approx 1.5$.

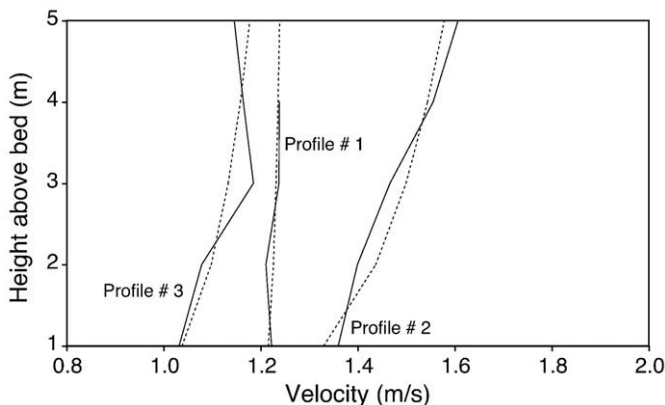


Fig. 6. Water velocity profiles for the three sampling verticals (solid lines), along with best-fits by the law of the wall (dashed lines, Eq. (7)). The law of the wall is reliable inside a layer extending from $z=0$ to approximately $z=0.2H$, where H is the total channel depth. For each of the three sampling verticals, water velocity profiles from the ADCP transect have been stacked in the lateral direction (ensemble averaging), over the twenty meters bracketing the sampling vertical. This spatial averaging allows to overcome the potential temporal, high-frequency fluctuations of recorded water velocity around the mean water velocity u .

This value can be compared to previous measurements of α compiled from the literature by Rutherford (1994). A large range of aspect ratios (from about 4 to 500) and flow configurations is spanned by these measurements. The value of α depends on the flow configuration (Fischer, 1976; Fischer et al., 1979; Rutherford, 1994). Natural channels display a large variability of α values, from 0.1 to 3.5, likely owing to the diversity of channel morphologies. For straight natural channels, $\alpha = 0.2\text{--}0.8$, with most of the values in the range $0.2\text{--}0.3$. For natural channels with meanders, $\alpha = 0.1\text{--}1.0$. Meanders thus increase the efficiency of lateral mixing. Finally, sharp bends seem to be the most efficient feature for increasing the lateral turbulent mixing in natural rivers, with $\alpha = 0.2\text{--}3.5$. The Solimões reach studied here has a rather high α , despite presenting only two relatively gentle bends. This can be attributed to the presence of islands and of sand dunes at the bottom of the Solimões River, which would tend to increase the efficiency of lateral mixing, for a given channel geometry. (Gaudet and Roy, 1995) also showed that channel depth differential between the two mixing tributaries (which obviously exists in the case of the Solimões–Purús confluence) can increase the efficiency of lateral mixing. The influence of bottom morphology and of the presence of islands on turbulent mixing in large rivers has to be further studied, to allow for a better prediction of dispersion rates and mixing length in these systems.

4.5. A predictive criterion for the occurrence of river lateral heterogeneities

The mean depth of the large Amazon tributaries reaches several tens of meters and their width a few kilometers. These length scales, combined with the compositional differences of tributaries, result in the flow of poorly-mixed water masses. In general, the persistence of chemical heterogeneities downstream from a confluence will depend on several geometrical and geomorphological features of the considered river. Dimensional analysis shows that the characteristic timescale T_{mix} necessary for turbulent mixing to homogenise water composition along the river width W , scales as:

$$T_{\text{mix}} = \frac{W^2}{\varepsilon_y}. \quad (8)$$

Significant lateral chemical heterogeneities of river water will be obtained for relatively long diffusion characteristic times T_{mix} with respect to the travel time of water:

$$T_{\text{mix}} \gg \frac{d}{u}, \quad (9)$$

with d the distance covered by the water flow at the mean velocity u during a given lapse of time. Using the scaling of ε_y (Eq. (6)), one finally obtains the criterion:

$$d \ll \frac{1}{\alpha} \cdot \frac{u}{u^*} \cdot W \cdot \frac{W}{H}. \quad (10)$$

The mixing length thus depends on the channel width, aspect ratio, flow structure, and various morphological features influencing α , as discussed above. Considering that in rivers, $u/u^* \approx 10$ (Chow, 1959), that large rivers have aspect ratios $W/H \approx 100$, and that measured lateral turbulent dispersion coefficients are lower than 5 (Rutherford, 1994):

$$d \ll 200 \times W. \quad (11)$$

For a typical large river having a width of 1 km, lateral chemical heterogeneities can be observed up to several tens of kilometers downstream from the confluence. This mixing length is valid for very “well-mixing conditions”, and thus constitutes a lower bound. Aspect

ratios larger than 100, as well as high mean longitudinal velocities compared to the shear velocity, will increase this mixing length. Finally, absence of bends, islands, or relatively smooth river beds (conditions that can be encountered especially in engineered channels) will also enhance the persistence of lateral chemical heterogeneities. These large mixing lengths agree well with chemical heterogeneities and large mixing lengths reported by Mackay (1970), Krouse and Mackay (1971), Stallard (1987), and Rathbun and Rostad (2004).

5. Conclusion

The Manacapuru sampling site on the Solimões River had been chosen to be a reference gauging station because it is apparently far from influence of any large tributaries. Nevertheless, major dissolved species and high-precision Sr isotopic ratios reveal lateral heterogeneities of river water composition in this cross-section. These heterogeneities are due to poor lateral mixing between two water masses, one from the Solimões mainstream, originating in the Andes, and having high dissolved species concentrations and non-radiogenic isotopic ratios; and the other supplied by the Purús River, derived from diluted and radiogenic lowland waters. Na⁺ concentration data allows for an estimate of the transverse dispersion coefficient of the considered Solimões reach. Dimensional analysis demonstrates that most large rivers are heterogeneous over a significant portion of their course (i.e. at least several tens of kilometers downstream confluences of tributaries having contrasted chemical signatures). This conclusion may appear obvious in cases of poor water mixing visible on satellite images (for instance between the Negro River and the Solimões River). Our study however sets up a more general conclusion for turbulent mixing of river waters and has important implications for representative river water sampling. Similar studies on large rivers confluences are necessary to yield supplementary constraints on turbulent mixing, and especially about the influence of complex geomorphological features such as bottom dunes and islands. High-precision Sr isotopes measurements can help to detect heterogeneities relatively far from confluences, or downstream from confluences of two tributaries having relatively close chemical signatures, increasing the number of potential sites to study transverse mixing in natural rivers.

Acknowledgements

The field campaign was supported by the French IRD, in the frame of the HyBAM Program (www.mpl.ird.fr/hybam/) with cooperation agreement with the Brazilian Research Centre (CNPq) no. 492685/2004–5. This program is developed in Brazil in cooperation with several Institutions and Universities (ANA, UnB, UFF, CPRM); we thank particularly P. Moreira-Turcq and all the staff of the C^{te} Cuadros ship for their help during the sampling campaign. We are grateful to C. Gorge, J.-L. Birck and P. Louvat for analytical help, and to O. Eiff, F. Métivier, R.G. Hilton and M. Albenque for helpful comments. This is IGP contribution 2569.

References

- Allègre, C.J., Hamelin, B., Provost, A., Dupré, B., 1987. Topology in isotopic multispace and origin of mantle heterogeneities. *Earth Planet. Sci. Lett.* 81, 319–337.
- Aucour, A.-M., Tao, F.X., Moreira-Turcq, P., Seyler, P., Sheppard, S., Benedetti, M.F., 2003. The Amazon River: behaviour of metals (Fe, Al, Mn) and dissolved organic matter in the initial mixing at the Rio Negro-Solimões confluence, 2003. *Chem. Geol.* 197, 271–285.
- Birck, J.-L., 1986. Precision K–Rb–Sr isotopic analysis: application to Rb–Sr chronology. *Chem. Geol.* 56, 73–83.
- Caplow, T., Schlosser, P., Ho, D.T., 2004. Tracer study of mixing and transport in the Upper Hudson River with multiple dams. *J. Hydr. Eng.* 130, 1498–1500. doi:10.1061/(ASCE)0733-9372(2004)130:12(1498).
- Chow, V.T., 1959. *Open-channel hydraulics*. McGraw-Hill, New York.
- Csanady, G.T., 1973. *Turbulent diffusion in the environment*. Dordrecht, Boston.
- Dunne, T., Mertes, L.A.K., Meade, R.H., Richey, J.E., Forsberg, B.R., 1998. Exchanges of sediment between the flood plain and channel of the Amazon River in Brazil. *Geol. Soc. Am. Bull.* 110 (4), 450–467.
- Dupré, B., Gaillardet, J., Rousseau, D., Allègre, C.J., 1996. Major and trace elements of river-borne material: the Congo Basin. *Geochim. Cosmochim. Acta* 60 (8), 1301–1321.
- Dupré, B., Viers, J., Durand, J.-L., Polvé, M., Bénézet, P., Vervier, P., Braun, J.-J., 1999. Major and trace elements associated with colloids in organic-rich river waters: ultrafiltration of natural and spiked solutions. *Chem. Geol.* 160, 63–80.
- Farlow, S.J., 1993. *Partial differential equations for scientists and engineers*. Dover, New York.
- N. Filizola, 2003. *Transfert sédimentaire actuel par les fleuves amazoniens*. PhD thesis, Université Toulouse III Paul Sabatier.
- Filizola, N., Guyot, J.-L., 2003. The use of Doppler technology for suspended sediment discharge determinations on the River Amazon at Óbidos. *Hydrol. Sci. J.* 49 (1), 143–153.
- Fischer, H.B., 1973. Longitudinal dispersion and turbulent mixing in open-channel flow. *Ann. Rev. Fluid Mech.* 5, 59–78.
- Fischer, H.B., 1976. Mixing and dispersion in estuaries. *Ann. Rev. Fluid Mech.* 8, 107–133.
- Fischer, H.B., List, J.E., Koh, C.R., Imberger, J., Brooks, N.H., 1979. *Mixing in inland and coastal waters*. Academic Press, London.
- Gaillardet, J., Dupré, B., Allègre, C.J., Négrel, P., 1997. Chemical and physical denudation in the Amazon River Basin. *Chem. Geol.* 142, 141–173.
- Gaillardet, J., Dupré, B., Louvat, P., Allègre, C.J., 1999. Global silicate weathering and CO₂ consumption rates deduced from the chemistry of large rivers. *Chem. Geol.* 159 (0), 2–30.
- Gaudet, J.M., Roy, A.G., 1995. Effect of bed morphology on flow mixing length at river confluences. *Nature* 373 (0), 138–139.
- Gerard, M., Seyler, P., Benedetti, M.F., Alves, V.P., Boaventura, G.R., Sondag, F., 2003. Rare earth elements in the Amazon basin. *Hydrol. Process.* 17, 1379–1392.
- Gibbs, R.J., 1967. Amazon River system: environmental factors that control its dissolved and suspended load. *Science* 156, 1734–1737.
- Goldstein, S.L., Jacobsen, S.B., 1984. The Nd and Sr isotopic systematics of river water dissolved material: implications for the sources of Nd and Sr in seawater. *Earth Planet. Sci. Lett.* 70, 221–236.
- Gualtieri, C., 2009. RANS-based simulation of transverse turbulent mixing in a 2D-geometry. *Environ. Fluid Mech.* doi:10.1007/s10652-009-9119-6.
- Huh, Y., Tsoi, M.-Y., Zaitsev, A., Edmond, J.A., 1998. The fluvial geochemistry of the rivers of Eastern Siberia I. Tributaries of the Lena River draining the sedimentary platform of the Siberian Craton. *Geochim. Cosmochim. Acta* 62 (16), 1657–1676.
- Krouse, H.R., Mackay, J.R., 1971. Application of H₂¹⁸O/H₂¹⁶O abundances to the problem of lateral mixing in the Liard–Mackenzie River system. *Can. J. Earth Sci.* 8 (9), 1107–1109.
- Mackay, J.R., 1970. Lateral mixing of the Liard and Mackenzie rivers downstream from their confluence. *Can. J. Earth Sci.* 7 (1), 111–124.
- Maurice-Bourgoin, L., Quemarais, B., Moreira-Turcq, P., Seyler, P., 2007a. Transport, distribution and speciation of mercury in the Amazon River at the confluence of black and white waters of the Negro and Solimões Rivers. *Hydrol. Processes* 17, 1405–1417.
- Maurice-Bourgoin, L., Bonnet, M.-P., Martinez, J.-M., Kosuth, P., Cochonneau, G., Moreira-Turcq, P., Guyot, J.-L., Vauchel, P., Filizola, N., Seyler, P., 2007b. Temporal dynamics of water and sediments exchanges between the Curuaí floodplain and the Amazon River, Brazil. *J. Hydrol.* 335, 140–156. doi:10.1016/j.jhydrol.2006.11.023.
- Meybeck, M., Ragu, A., 1996. River discharge to the oceans. An assessment of suspended solids, major ions and nutrients. Environment information and assessment UNEP/WH, UNEP, Nairobi.
- Meynadier, L., Gorge, C., Birck, J.-L., Allègre, C.J., 2006. Automated separation of Sr from natural water samples or carbonate rocks by high performance ion chromatography. *Chem. Geol.* 227, 26–36.
- Molinier, M., Guyot, J.-L., De Oliveira, E., Guimarães, V., 1996. Les régimes hydrologiques de l'Amazonie et de ses affluents, vol. 238. IAHS Publication, pp. 209–222.
- Moreira-Turcq, P., Seyler, P., Guyot, J.-L., Etcheber, H., 2003. Characteristics of organic matter in the mixing zone of the Rio Negro and Rio Solimões of the Amazon River. *Hydrol. Process.* 17, 1393–1404.
- Mortatti, J., Probst, J.-L., 2003. Silicate rock weathering and atmospheric/soil CO₂ uptake in the Amazon basin estimated from river water chemistry: seasonal and spatial variations. *Chem. Geol.* 197, 177–196.
- Pope, S.B., 2008. *Turbulent flows*. Cambridge Univ. Press.
- Rathbun, R.E., Rostad, C.E., 2004. Lateral mixing in the Mississippi River below the confluence with the Ohio River. *Water Resour. Res.* 40, W05207. doi:10.1029/2003WR002381.
- Rutherford, J.C., 1994. *River Mixing*. J. Wiley & Sons, New York. 336 pp.
- Seyler, P.T., Boaventura, G.R., 2003. Distribution and partition of trace metals in the Amazon basin. *Hydrol. Process.* 17, 1345–1361.
- Sioli, H., 1984. The Amazon and its main affluents: hydrography, morphology of the river courses, and river types. In: Sioli, H. (Ed.), *The Amazon: Limnology and Landscape Ecology of a Mighty Tropical River and its Basin*. Dordrecht, pp. 127–165.
- Stallard, R.F., 1987. Cross-channel mixing and its effect of sedimentation in the Orinoco River. *Water Resour. Res.* 23 (10), 1977–1988.
- Stallard, R.F., Edmond, J.M., 1983. Geochemistry of the Amazon 2. The influence of geology and weathering environment of the dissolved load. *J. Geophys. Res.* 88 (C14), 9671–9688.
- Taylor, G., 1954. The dispersion of matter in turbulent flow through a pipe. *Proc. Roy. Soc. London* 223 (1155), 446–468.
- Tritton, D.J., 1988. *Physical Fluid Dynamics*. Clarendon Press, Oxford. 536 pp.
- Vanoni, V.A., 2006. Sediment transportation mechanics. In: Vanoni, V.A. (Ed.), *Sedimentation engineering*. EWRI, pp. 11–190.
- Viers, J., Barroux, G., Pinelli, M., Seyler, P., Oliva, P., Dupré, B., Boaventura, G.R., 2005. The influence of the Amazonian floodplain ecosystems on the trace elements dynamics of the Amazon River mainstem (Brazil). *Sci. Total Environ.* 339, 219–232.
- Yotsukura, N., Sayre, W.W., 1976. Transverse mixing in natural channels. *Water Resour. Res.* 12, 695–704.